Commun. Comput. Phys.
doi: 10.4208/cicp.OA-2019-0157

Vol. **28**, No. 3, pp. 1019-1037
September 2020

Accelerated Molecular Statics Based on Atomic Inertia Effect

Fei Shuang[1,2], Pan Xiao[1,*], Yilong Bai[1] and Fujiu Ke[3]

[1] *LNM, Institute of Mechanics, Chinese Academy of Sciences, Beijing 100190, China.*
[2] *Department of Mechanical and Aerospace Engineering, University of Florida, Gainesville, FL, 32611, USA.*
[3] *School of Physics and nuclear energy engineering, Beihang University, Beijing 100191, China.*

Received 6 September 2019; Accepted (in revised version) 28 November 2019

Abstract. Molecular statics (MS) based on energy minimization serves as a useful simulation technique to study mechanical behaviors and structures at atomic level. The efficiency of MS, however, still remains a challenge due to the complexity of mathematical optimization in large dimensions. In this paper, the Inertia Accelerated Molecular Statics (IAMS) method is proposed to improve computational efficiency in MS simulations. The core idea of IAMS is to let atoms move to meta positions very close to their final equilibrium positions before minimization starts at a specific loading step. It is done by self-learning from historical movements (atomic inertia effect) without knowledge of external loadings. Examples with various configurations and loading conditions indicate that IAMS can effectively improve efficiency without loss of fidelity. In the simulation of three-point bending of nanopillar, IAMS shows efficiency improvement of up to 23 times in comparison with original MS. Particularly, the size-independent efficiency improvement makes IAMS more attractive for large-scale simulations. As a simple yet efficient method, IAMS also sheds light on improving the efficiency of other energy minimization-based methods.

AMS subject classifications: 74G65, 74A25, 74S30

Key words: Molecular statics, energy minimization, local optimization, efficiency improvement.

1 Introduction

Over the past two decades, intensive research interests have been dedicated in nanomechanics and nanomaterials to uncover underlying deformation mechanisms resulting

*Corresponding author. *Email addresses:* xiaopan@lnm.imech.ac.cn (P. Xiao), shuangfei@ufl.edu (F. Shuang), baiyl@lnm.imech.ac.cn (Y. Bai), kefj@lnm.imech.ac.cn (F. Ke),

from individual atoms [1–4]. In particular, well-developed atomistic simulation methods such as molecular dynamics (MD) [5], molecular statics (MS) [6], Monte Carlo (MC) [7] and nudged elastic band (NEB) calculation [8] are of great importance to predict material properties and explain deformation mechanisms, which provide alternative research tools besides in situ experiments. Among these methods, empirical-based methods greatly reduce the computational cost and make simulations with millions of atoms possible [9]. Currently, empirical-based MD and MS are two of the most commonly used methods which are capable of dealing with more than 10^8 atoms with simple potential models like Lennard-Jones (LJ) and embedded atomic model (EAM), achieving the great accomplishment in studying nanomaterials [10] and manipulating their properties [11]. Despite the successful development of modern computer technology and new numerical algorithms, it is always important to improve computational efficiency as much as possible in order to shorten research period and increase simulation dimension.

Various methodologies have been developed to improve simulation efficiency from the perspectives of physics and mathematical optimization. Physically, one can develop new methods to bridge across length and time scale gap between MD and continuum theory. Long timescale dynamics such as EON [12] and diffusive MD [13] can be used in simulations of experimental timescale events. One of the extreme situations is quasi-static simulation at finite temperature without strain rate effect. Molecular Statistical Thermodynamics (MST) [14] and Engineering Molecular Mechanics (EMM) [15] are two representative work. Based on the local harmonic approximation [16], MST uncouples atomic motion from thermal vibration with high frequency. The Helmholtz free energy instead of potential energy is minimized to search local stable configuration at finite temperature. MST shows excellent efficiency improvement and reliable results in simulations of copper nanowire tensile, thin film nanoindentation and phase transformation of ZnO nanowires [14]. For EMM method, parameters of interatomic potential are considered temperature-dependent and are modified as functions of simulating temperature. EMM shows good agreement with conventional MD when simulating elastic properties and thermal stress with 100 times improving efficiency, but the feasibility of EMM on plastic deformation simulation is unknown.

On the other hand, several multi-scale methods based on energy minimization have been proposed in the last few decades to decrease the computational cost of ultra-large atomistic systems [17]. Hierarchically, FE2AT utilizes information from finite element calculation to provide appropriate initial and boundary conditions for atomistic simulations, such that large parts of the elastic loading process can be accelerated [18]. Concurrently, atomistic representation is used in regions under inhomogeneous deformation dominated by dislocation evolutions, whereas quasi-continuum representation is used in regions under homogeneous deformation to reduce computational cost. One of the typical multi-scale methods is the quasi-continuum (QC) method which searches for the positions of representative nodes by minimizing the coarse-grained potential energy [19]. By introducing discrete dislocation line in QC framework, coupled atomistics and discrete dislocation mechanics (CADD) was put forward further to improve the efficiency

in simulations of nanoindentation [20] and crack propagation [21]. Recently, CADD has been extended into 3 dimension successfully [22].

Besides the efforts on designing new algorithms by using some physical approximations, some researchers focus on developing new minimization algorithms, such as the fast inertial relaxation engine method (FIRE) [23, 24], NVERE [25] and preconditioners for the geometry optimization [26]. Developing new optimization algorithms for large scale molecular simulations is more challenging when we look back the history of mathematical optimization. The background of physics, however, endows minimization with more understandable meanings for mathematical terminologies and operations such as position, velocity, energy, force and dynamics matrix. Therefore, combination of physical knowledge and mathematical algorithm could be an effective way to develop a new method with higher efficiency.

In this paper, we intend to develop an accelerated MS method based on atomic inertia effect named Inertia Accelerated Molecular Statics (IAMS). Our method shows promising efficiency improvement in comparison with original MS with very less extra computational burden and difficulty of code implementation, regardless of shapes, boundary conditions and preexisting defects. The size-independent efficiency also makes IAMS very attractive for large-scale simulations. The rest of the paper is organized as follows. In Section 2, energy minimization algorithms and relevant simulation settings are presented. In Section 3, efficiency improvement by elastic mapping loading in simulations of 1D atomic chain and 2D atomic bar is analyzed to point out the key of accelerated MS simulations. The theory of the method and various applications are given in Section 4. The efficiency analysis and discussion are presented in Section 5. Finally, in Section 6 we conclude the paper with a brief summary.

2 Methods

In traditional MS simulations, total potential energy of the system at each loading step is minimized. Conjugate gradient (CG) method is a typical and commonly used algorithm for the minimization process. In CG algorithm, atomistic position vector ($\mathbf{x}_{k+1}$) is updated according to the current conjugate direction ($\mathbf{d}_k$) and step size (α_k):

$$\mathbf{x}_{k+1} = \mathbf{x}_k + \alpha_k \mathbf{d}_k, \tag{2.1}$$

where k indicates the iteration step. $\mathbf{d}_k$ is calculated from atomistic force vector $\mathbf{f}_k$ and searching direction. At each loading step, there will be different number of iteration steps (n_{iter}) which is related to characteristics of energy profiles. At iteration step k, α_k is determined through line-searching methods in which the systems energy and atomistic force vector needs to be evaluated for several times (n^k_{line}). Therefore, the total times of energy and force evaluation (n_{eval}) at a loading step is

$$n_{eval} = \sum_{k=1}^{n_{iter}} n^k_{line}. \tag{2.2}$$

For the force-based criterion adopted in this paper, the system is assumed to reach an equilibrium state when the resolution criterion (ϵ) of minimization is satisfied:

$$\sum_i \left| f_k^i \right| / N < \epsilon, \quad i = 1,2,\cdots,N, \tag{2.3}$$

where N is the atom number, $\left| f_k^i \right|$ is the force magnitude of atom i at k iteration step. In this work, ϵ with value of 1×10^{-4} eV/Å is used to assure the accuracy of energy minimization except when different precisions are the concern.

Two types of empirical potentials are used in this paper. The first one is Lennard-Jones (LJ) potential with form:

$$V(r) = 4\epsilon\left[\left(\frac{\sigma}{r}\right)^{12} - \left(\frac{\sigma}{r}\right)^{6}\right], \tag{2.4}$$

where $\epsilon = 0.4916$ eV and $\sigma = 2.60$ Å for copper (Cu). LJ potential is used to describe interatomic force for 1-dimensional (1D) atom chain, 2-dimensional (2D) compression and 2D nanoindentation with hex lattice. The embedded atom model (EAM) developed by Foiles et al. [27] is used to describe atomic interactions of Cu atoms in three-point bending simulations.

OVITO is used to visualize atomistic configuration [28]. The common neighbor analysis (CNA) [29] and centro-symmetry parameter (CSP) [30] are used to identify defect atoms.

3 MS with mapping loading

3.1 Tension of atom chain model

Fig. 1 shows the 1D atom chain with single freedom degree. Atom 1 is fixed, atom 2 is active and atom 3 is used for loading. There are two commonly used loading operations in molecular simulations: direct and mapping. In direct loading, atom 3 will move to the right with distance δ. In mapping loading, atom 3 will move to the same position as in direct loading, but atom 2 will be placed at the middle point of atom 1 and atom 3 based on the simple mapping rule $x_2 = (x_1 + x_3 + \delta)/2$. In both loading modes, atom 1 is always fixed to avoid the chain translation, and atom 2 will move driven by unbalanced force during the minimization process until the given convergence precision is met.

Tensile simulations of the atom chain were performed using the two loading modes respectively, and relevant results are presented in Fig. 2. For the force-displacement curves in Fig. 2(a), two simulations coincide until B. The force of mapping loading decreases slowly after B, whereas the force of direct loading decreases quickly with an abrupt drop at B. Potential profiles of the atomic system at different displacement are also given in the insets of Fig. 2(a). At point A, the potential landscape has a single local minima, and atom 2 in the two simulations locates at the bottom of the well. At point B, there are two shallow potential wells with local minima. After convergence, atom 2 using mapping loading stays on saddle point while atom 2 using direct loading lies at the bottom

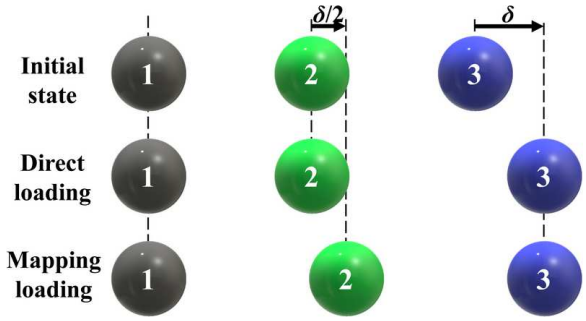

Figure 1: Initial state and two loading modes of 1D atom chain.

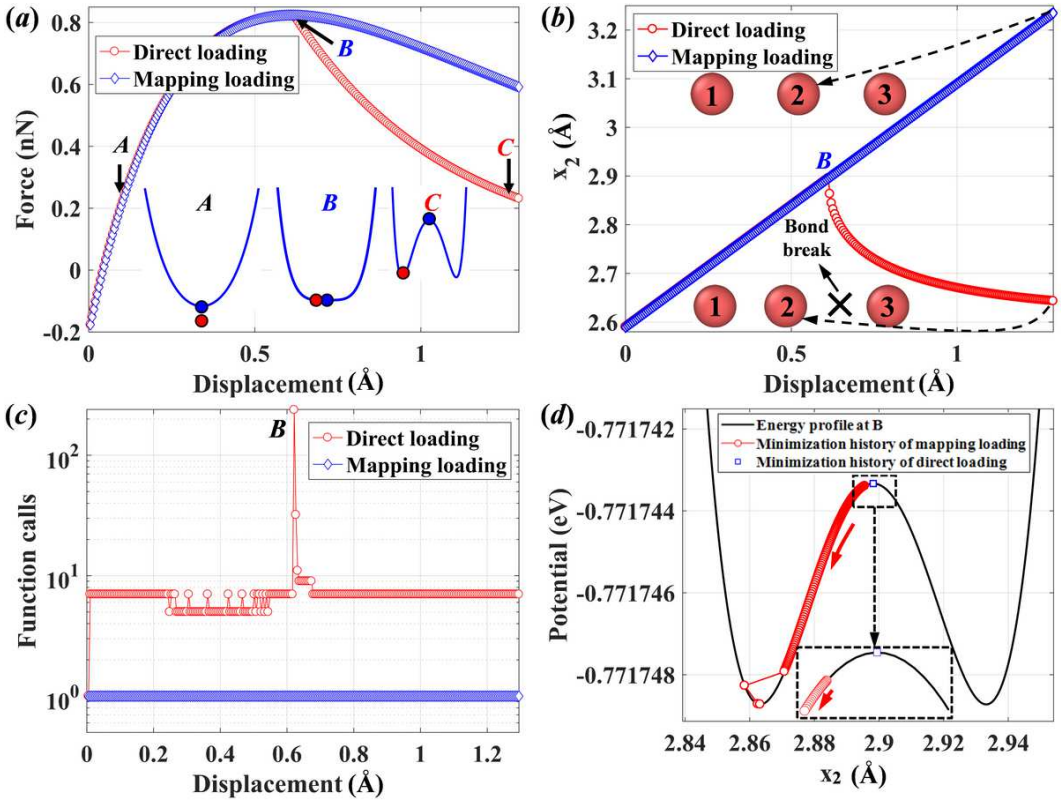

Figure 2: Comparison of two loading modes for (a) stress-strain curves and evolution of potential energy profiles at different states, (b) position of active atom 2 during the tensile simulation, (c) computational cost and (d) minimization history near point B.

of the left well. Atom 2 starts to move towards atom 1 after B with direct loading, indicating the bond break between atom 2 and 3 as shown in Fig. 2(b). On the contrary, atom chain with mapping loading deforms as a super-elastic chain without fracture. Fig. 2(c) gives the computational cost in terms of function calls during the minimization process.

Simulation using mapping loading is much faster than that of direct loading. Only one function call is needed to converge in mapping loading, but around 7 function calls are needed in direct loading for normal loading steps. Particularly, more than 200 function calls are required to terminate the iterations at B. Fig. 2(d) presents the atomistic trajectories of atom 2 during the minimization processes with two loading styles at B. After mapping loading, atom 2 lies exactly at saddle point of potential and thus no unbalanced force drives it to move. However, as the potential profile is changed by direct loading, atom 2 lies at the left side of the saddle point, resulting in the migration towards left well bottom driven by unbalanced force. The long distance migration from one well bottom to the other needs much more iterations than normal steps, which leads to the huge computational cost difference between step B and normal steps. Therefore, the loading mode affects not only the deformation mechanism but also the computational cost, and mapping loading can effectively improve the efficiency. It is worth noting that after point B in mapping loading, atom 2 locates at a metastable position in the potential landscape, and any small disturbance to atom 2 will let it move to one of the minima. However, the metastable solution obtained from mapping loading can be avoided by introducing some factitious disturbance.

3.2 Compression of 2D atomic system

As the essence of the two different loading modes is depicted in the 1D atom model, here a more realistic 2D atomic model is considered to study the collective behavior of atoms under different loading styles. The corresponding 2D atomistic configuration is given in the inset of Fig. 3(a) with the similar definition of fixed, active and loading atoms. Direct loading here is the same as in 1D atom chain, and mapping loading follows a more complex rule. In mapping loading, all the active atoms will be mapped to new positions based on:

$$x_{\text{active}}^{\text{new}} = x_{\text{active}}^{\text{old}} + \frac{x_{\text{active}}^{\text{old}} - \min(\mathrm{x}_{\text{active}}^{\text{old}})}{\max(\mathrm{x}_{\text{active}}^{\text{old}}) - \min(\mathrm{x}_{\text{active}}^{\text{old}})}. \tag{3.1}$$

Fig. 3(a) plots the force-displacement curves. Two loading modes have the same response until A. Force of direct loading drops firstly at A and then increases, while force of mapping loading drops relatively later at B and further at C and then increases, indicating that direct loading advances the initial dislocation nucleation. Again, as plotted in Fig. 3(b), results of mapping loading show the promising efficiency improvement (about 10 times faster than that of direct loading in average) at most loading steps except points B and C with dislocation nucleations.

Fig. 4 shows snapshots of atomic configuration colored by force magnitude during minimization process. As the direct loading is imposed, the loading effect propagates from right side to left layer by layer as indicated by the non-equilibrium force distribution in Fig. 4(a) to Fig. 4(c). After that, the system reaches to an equilibrium state as shown in Fig. 4(d). A lot of minimization iterations are used for the propagation process.

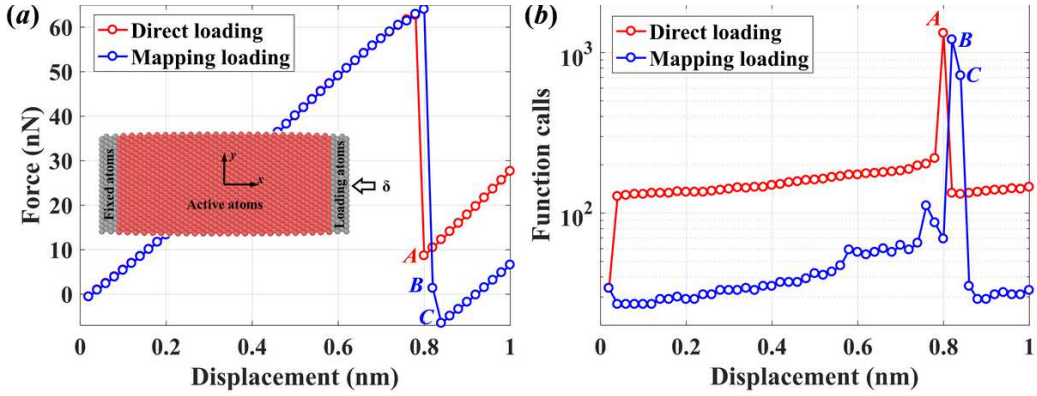

Figure 3: Comparison of two loading modes in (a) stress-strain curves and (b) computational cost. Inset figure of (a) gives the configuration of the 2D atom bar under compression.

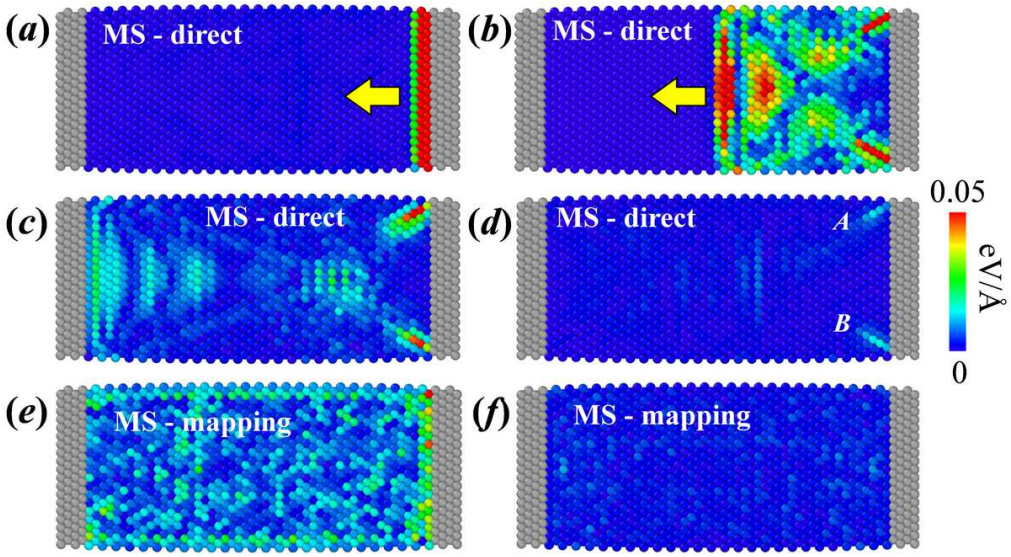

Figure 4: Evolution of atomic force during MS minimization with direct loading ((a)-(d)) and MS with mapping loading ((e)-(f)).

While in mapping loading mode, the non-equilibrium force due to compressive loading can be mapped onto all atoms instantaneously at the beginning, and the layer-by-layer propagation process can be avoided, as shown in Fig. 4(c) and Fig. 4(d). Therefore, a lot of computational cost can be saved.

After convergence, atoms at A and B with higher force are relatively unstable in Fig. 4(d) because they are close to the loading side. Our simulations show that dislocations will nucleate from A and B. Atoms in Fig. 4(f), however, with uniform and small forces after convergence make the system more stable, which can explain why mapping loading can avoid premature dislocation nucleation.

The simulation results from 1D and 2D atomic systems reveal that a key to effectively improve efficiency of MS is to find an atomistic configuration as close as possible to its optimal state at a specific loading step, as done by the mapping loading. However, there is no simple rules to apply mapping loading to configurations with complex shapes, defects or boundary conditions. Even for simple loading like tensile or compression, mapping loading based on conventional elastic solution cannot handle surface inhomogeneity in nanoscale [31]. Therefore, it is quite necessary to develop a new algorithm with more generality and high efficiency to accelerate MS simulations based on the ideology of mapping loading.

4 Accelerated MS based on atomic inertia effect

Here the Inertia Accelerated Molecular Statics (IAMS) is proposed to overcome the limitation of mapping loading and improve the efficiency further. It is expected to be effectively applied in most energy minimization based methods with discrete nodes, particles and/or coupled systems (multiscale method like QC [19] and CADD [20]). In this section, computational procedure and efficiency of the IAMS will be presented along with MS in some classical applications.

4.1 Methodology of IAMS

For a given molecular system, no matter what atomic type and interatomic potential are, it usually shows similar response when facing similar external loadings, especially when the timescale of external loadings is much larger than that of atomic thermal motions. That is, most atoms in the system may behave like their last movement due to inertia effect. Therefore, the core idea of IAMS is to let atoms move by self-learning from historical movements without knowledge of external loadings. Specifically, for an arbitrary atom in the configuration shown in Fig. 5, assume its equilibrium position at loading step $k-1$ and k are x_{k-1} and x_k, the displacement $d_{k-1}=x_k-x_{k-1}$ can be considered as the response of this atom to the $(k-1)^{\text{th}}$ external loading step. Under the next similar k^{th} external loading step, the atom is expected to have the similar response of d_{k-1}, such that the new equilibrium position can be predicted as

$$x'_{k+1}=d_{k-1}+x_k=2x_k-x_{k-1}. \tag{4.1}$$

The vector form for predicting positions of all atoms at loading step $k+1$ can be written as

$$\mathbf{X}'_{k+1}=2\mathbf{X}_k-\mathbf{X}_{k-1}. \tag{4.2}$$

Fig. 6 gives the flow charts of three MS methods: MS with direct loading, MS with mapping loading based on the knowledge of elastic deformation (denoted as EAMS) and, the IAMS. It is worth noting that IAMS may fail to decrease energy when the system

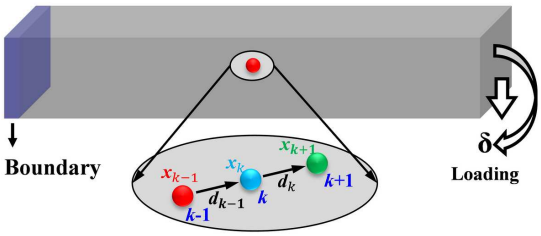

Figure 5: Schematic of the movement of an atom due to inertia effect in IAMS method.

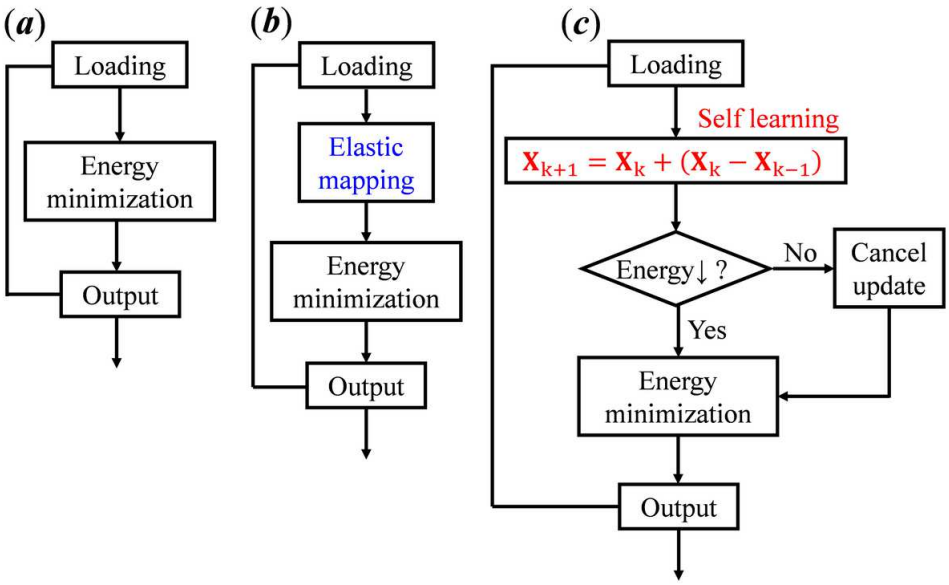

Figure 6: Flow charts of (a) conventional MS, (b) MS with mapping loading based on the knowledge of elastic deformation and (c) IAMS.

becomes unstable, so an energy monitor is used to check whether the system goes uphill. If the energy increases, inertia update must be cancelled and IAMS will degenerate to conventional MS, and the situation will be discussed in following applications. It is quite easy to implement IAMS into existing software codes without extra computational burden.

4.2 Applications of IAMS

4.2.1 Compression of 2D atomic system

In order to compare the efficiency of three methods in Fig. 6, compression simulation of 2D configuration in Section 3 was also performed with IAMS. As shown in Fig. 7(a), IAMS exhibits similar force-displacement response as the former two methods. The ini-

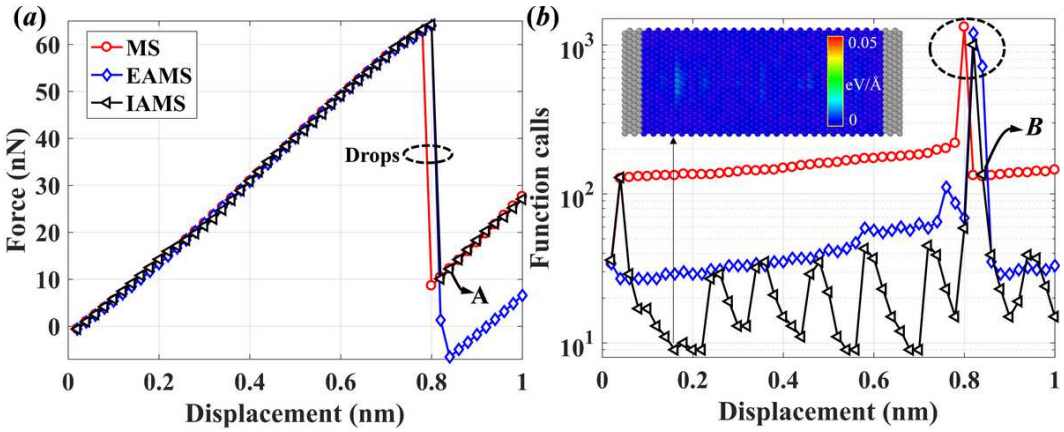

Figure 7: Comparison of the three methods: (a) force-displacement curves and (b) computational cost.

tial force drop of IAMS is the same as that of EAMS, but is slight later than that of MS, indicating that inertia update delays the premature dislocation nucleation as EAMS does. The computational cost shown in Fig. 7(b) highlights the efficiency superiority of IAMS. Even though EAMS speed up about 10 times in comparison with MS, IAMS reduces the computational cost further to half of that of EAMS in average. The inset figure of Fig. 7(b) presents the snapshot of atomic force magnitude after self-learning from previous steps. The system is much closer to the final equilibrium state compared with Fig. 4(e) after elastic mapping, which can explain the better efficiency of IAMS. Near the loading step at A, there is no efficiency improvement with IAMS due to dislocation events. Nonetheless, IAMS shows the reliable results with higher efficiency.

4.2.2 Three-point bending of nanopillar

The advantage of IAMS over EAMS lies not just in higher efficiency, but also in generality. Fig. 8(a) shows three different nanopillar configurations: single crystal with round section, nanotwinned pillar with round section and, single crystal with hexagonal section, respectively. The spacing between twin boundaries (TBs) is 2.08 nm. The three-point bending setup is illustrated in Fig. 8(b). Atoms at the two ends with thickness of 2.00 nm are fixed. Atoms in the middle section with thickness of 1.00 nm are moved downwards step by step to simulate the bending load. For the nanopillars with various shapes and intrinsic defects, it is difficult to find corresponding elastic solution even under simple loading as bending and torsion, therefore, only simulations with the conventional MS and IAMS were performed. CNA is used to identify atomic structures [30] after deformation as shown in Fig.8 (c). The deformed configurations from MS and IAMS simulations are quite similar except for the premature dislocations. Force-displacement curves from both MS and IAMS in Fig. 8(d) demonstrate the reliability of IAMS for complex configurations. Computational cost in Fig. 8(e) shows that simulations of IAMS are much faster than that of MS. Notably, the maximum efficiency improvement is up to about 23 times

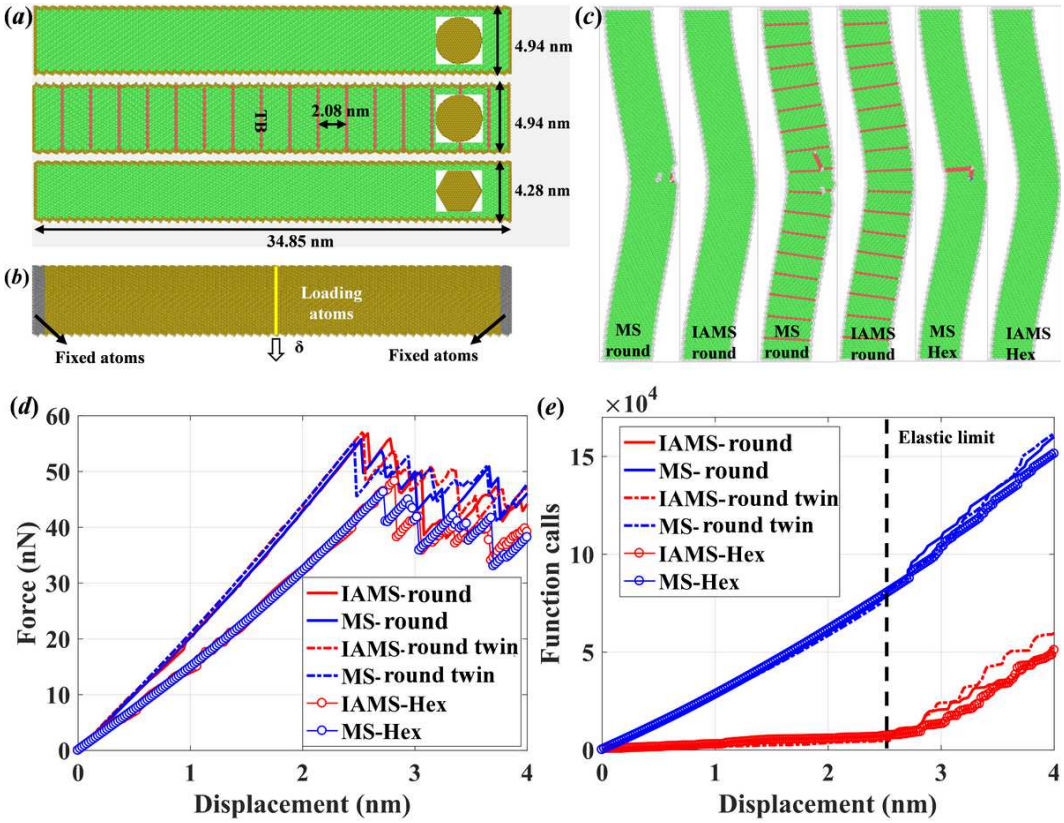

Figure 8: (a) Atomic configurations of single crystalline with round cross section, nanotwinned pillar with round cross section and, nanopillar with hexagonal cross section; (b) schematic of three-point bending setup; (c) deformed configurations, (d) force-displacement curves and (e) computational cost from different methods.

before elastic limit. After dislocation nucleations, the computational cost gap between the two methods stays almost the same, indicating IAMS has less efficiency improvement in the case of plastic deformation.

4.2.3 Nanoindentation of 2D atomic system

Above examples show that IAMS improves much the efficiency in elastic deformation but less in plastic deformation due to dislocations. Therefore, it is necessary to investigate its efficiency in a more complex deformation case like nanoindentation in which dislocation nucleation and interaction dominate almost the whole process. Fig. 9(a) and (b) show the initial and final snapshot of nanoindentation simulations using MS and IAMS. Atoms in the snapshots are colored by CSP to identify dislocations. Atoms at the bottom layers with thickness of 2.00 nm are fixed to avoid vertical translation. Periodic and free boundary conditions are imposed on x and y directions respectively. Results of the two methods show similar pile-up dislocations, showing that IAMS can effectively capture the related dislocation nucleation and evolution. Force-depth curves in Fig. 9(c)

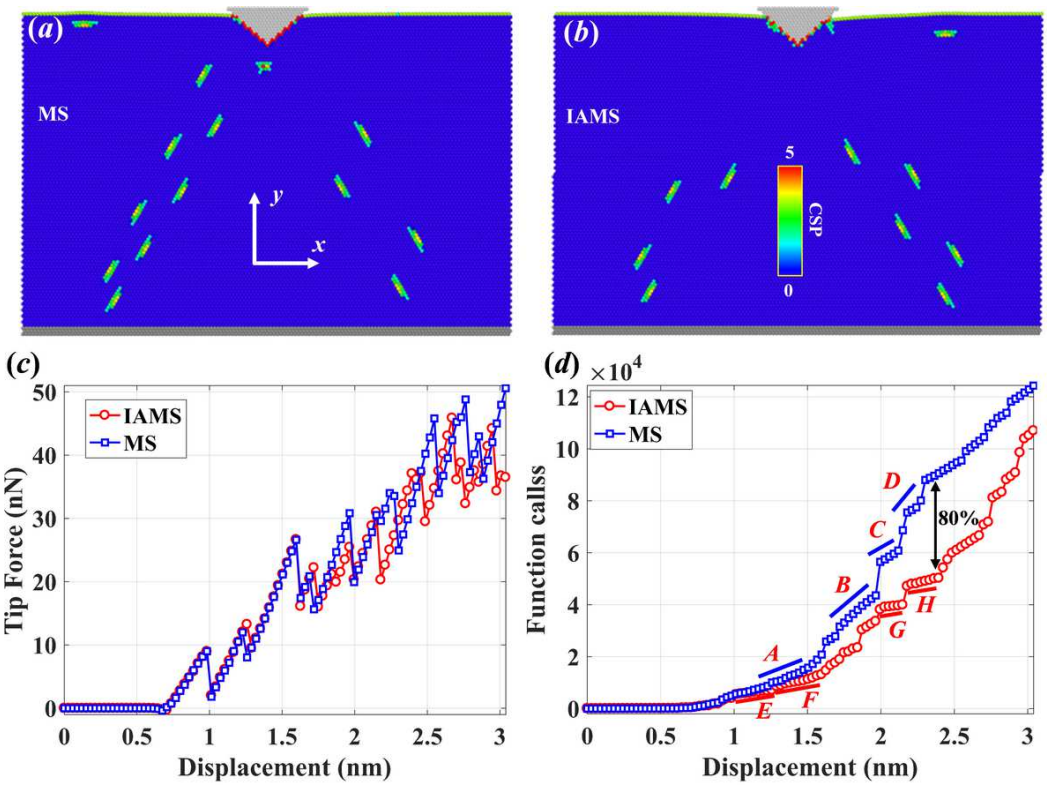

Figure 9: 2D Configurations of nanoindentation from (a) MS and (b) IAMS simulations; (c) force-displacement curves and (d) computational cost of MS and IAMS simulations.

from IAMS and MS simulations present similar trend with frequent drops due to dislocation events. The computational cost shown in Fig. 9(d) indicates that IAMS still needs less function calls than MS, and the maximum efficiency improvement is about 80% at the displacement of 2.40 nm. Function calls have similar jumps in Fig. 9(d) as the force drops in Fig. 9(c) due to dislocation events, which reduce the efficiency improvement of IAMS. However, slope of function calls in ranges between two jumps in IAMS is smaller than that in MS, resulting in the efficiency improvement of IAMS.

5 Discussion

5.1 Efficiency improvement of IAMS

As mentioned in Section 4.2, inertia update can speed up MS simulations 23 times without loss of fidelity. To get a more quantitative understanding of the efficiency improvement of IAMS, the efficiency improvement of IAMS is analyzed based on one loading step of the three-point bending simulation in Section 4.2.2. The improved efficiency of IAMS compared with MS is defined as $\eta = N_{\mathrm{MS}}/N_{\mathrm{IAMS}}$ which is plotted in Fig. 10(a) with

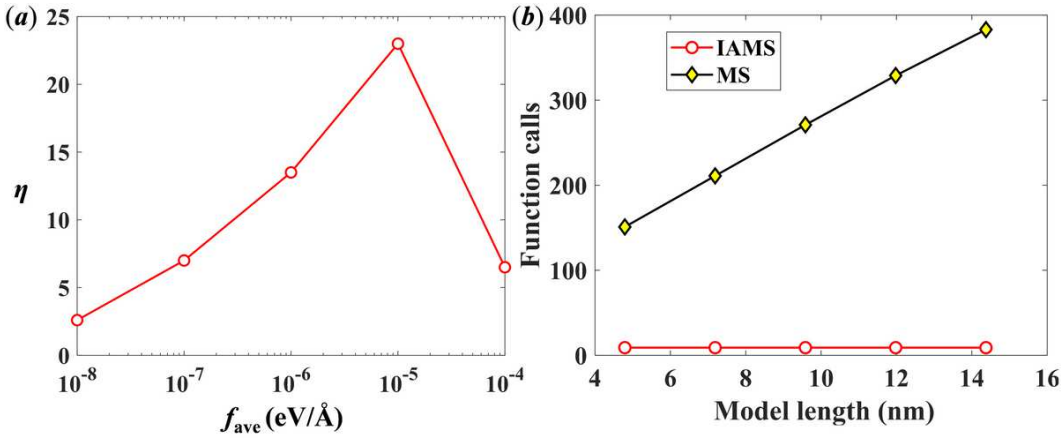

Figure 10: (a) Dependence of efficiency improvement () on convergence precision obtained from the three-point bending simulations with IAMS; (b) dependence of computational cost on model size in 2D bar compression simulations with MS and IAMS.

respect to different convergence precisions (ϵ). The lowest ϵ is set as 1×10^{-4} eV/Å to assure the reliability of simulations. It can be seen that the efficiency improvement is highly dependent on ϵ. The maximum η reaches to 23 times at $\epsilon = 1\times10^{-5}$ eV/Å, which means there exists an optimal precision with the highest efficiency improvement. It is known that computational cost of MS (n) depends on precision ϵ and model size ($L_{\max}$) for CG minimization as [32]:

$$n \propto \frac{L_{\max}}{a}|\log(\epsilon)|, \tag{5.1}$$

where a is a typical inter-atomic distance. This relation indicates that more computation cost is required for simulations with higher precision and larger size. When the precision ϵ is relatively low, the experience from previous step is not so accurate and will misleads the system evolution after inertia update, and thus extra computation is needed to fix the wrong attempt. When the precision is relatively high, the inertia based experience is good enough to predict the next movement, and thus less computation is needed. Increasing the precision further, however, the self-learned experience is more accurate, but not enough for the same precision in next step due to computational round-off error, leading to the decrease of efficiency improvement. Therefore, it is the competition between information loss with inertia update and the given precision that controls the efficiency improvement of IAMS.

The other important advantage of IAMS over MS is the size-independent computational cost as shown in Fig. 10(b). When the length of the 2D bar under compression in Section 4.2.1 was increased, the computational cost of MS increases linearly which is in agreement with Eq. (5.1), whereas computational cost of IAMS keeps constant, indicating the efficiency improvement will increase linearly with the size of the model. The different size dependence of IAMS and MS on computational cost can be explained from Fig. 4 and the inset of Fig. 7(b). In MS simulations, non-equilibrium forces propagate

from the loading side to the other side layer by layer as shown in Fig. 4, so the larger the length is, the more computational cost is needed. IAMS however, successfully avoids such size-dependent process by inertia update and maximizes the efficiency improvement. Therefore, the size-independent efficiency is another beneficial property of IAMS.

Applications of IAMS also indicate that efficiency improvement is primary from stages of elastic deformation. The efficiency improvement is not obvious when the system become an unstable state, e.g. atomic bond rearrangement due to dislocation nucleation and propagation and fracture, which is a local unstable event in atomic scale [1,33,34]. Although there are some theories for predicting dislocation nucleation, they are not suitable for describing system evolution in atomistic scale. Moreover, dislocation propagation is path-dependent which needs repeated trial by searching the lower energy path [35]. Therefore, it is hard to accelerate MS in dislocation evolution by utilizing atomic inertia effect, and IAMS will degenerate to MS in these cases. However, similar strategy can be applied in grain-scale methods such as discrete dislocation in dislocation dynamic (DD) simulations [36] to improve efficiency.

5.2 High-order IAMS

The proposed IAMS is similar to the predictor-corrector operation in solving ordinary differential equations (ODE) [37]. The similar strategy is also used in Limited memory BFGS method [38] in which the experience from last m steps is used to approximate the Hessian matrix. Accordingly, IAMS algorithm can be extended by learning more information from previous steps. Currently, operation of IAMS can be considered as one-order dynamics equation:

$$\widetilde{\mathbf{X}}_i(k+1)=\mathbf{X}_i(k+1)+\mathbf{v}_i(k+1). \tag{5.2}$$

If two-order dynamics is considered, the update equation can be expressed as:

$$\widetilde{\mathbf{X}}_i(k+1)=\mathbf{X}_i(k+1)+\mathbf{v}_i(k+1)+\frac{1}{2}\mathbf{a}_i(k+1), \tag{5.3}$$

where $\mathbf{v}$ and $\mathbf{a}$ can be obtained from history of atomic positions:

$$\mathbf{v}_i(k)=\mathbf{X}_i(k)-\mathbf{X}_i(k-1), \tag{5.4}$$

$$\mathbf{a}_i(k)=\mathbf{v}_i(k)-\mathbf{v}_i(k-1)=\mathbf{X}_i(k)-2\mathbf{X}_i(k-1)+\mathbf{X}_i(k-2). \tag{5.5}$$

The high-order IAMS is expected to accelerate nonlinear elastic deformation such as nanoindentation of 2D materials (such as graphene [39,40] and MoS2 [41–43]). Fig. 11(a) illustrates the linear force-displacement curve with inertia update strategy for one-order IAMS. In this situation, the trajectories of atoms are almost straight sections, and thus one-step experience is enough to predict the next movement. For large nonlinear deformation, however, atoms move along the curve with nonlinear directions and distances as shown in Fig. 11(b). The two-order IAMS would transfer more information of moving direction and distance with higher efficiency improvement for nonlinear deformation.

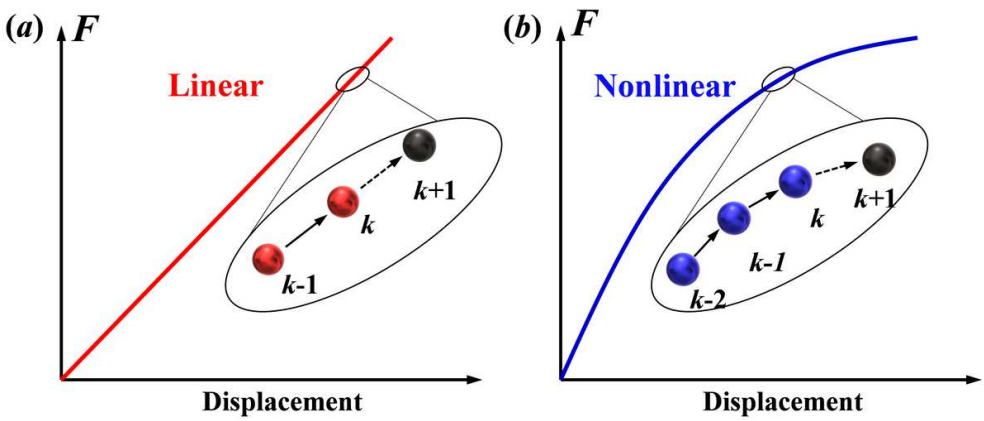

Figure 11: Schematic of IAMS for (a) linear and (b) nonlinear problems.

5.3 Comparison with path following methods and the significance of IAMS

Notably, the basic idea of IAMS is similar to path following methods (PFM) or numerical continuation, which are well-developed in solving nonlinear ODE equations, nonlinear eigenvalue problems [44] and bifurcation problems [45]. In particular, PFMs are also widely used to solve engineering problems such as quasi-static nonlinear structural [46] and fracture problems [47, 48] through finite element methods (FEM). It is known that FEM is usually solved by Newton-Raphson method with available Hessian matrix, while MS simulations need to search local energy minima with million or even billion degree of freedoms [38]. Due to the nonlocal interatomic force of atoms, it is computationally expensive for MS to utilize Hessian matrix in higher-order optimization algorithms and as a result, MS simulations are very sensitive to initial configuration and very time-consuming [49]. From the viewpoint of mathematics, therefore, FEM and energy minimization in MS simulations are two different applications. Though PFMs have been widely used in nonlinear structural and fracture problems, it doesn't mean these methods are applicable for large-scale atomistic simulations using energy minimization. The significance of IAMS is that atomic self-learning strategy by inertia effect (or path following method) is shown to be applicable to MS simulations for the first time, which becomes more exciting for researchers who work on computational nanomechanics because considerable time and economic cost can be saved with very less extra burden.

Besides improving efficiency, another contribution of IAMS is overcoming some issues of previous MS methods. For example, IAMS can avoid premature dislocation nucleation by moving the system to a more reasonable initial configuration. IAMS can effectively accelerate molecular statics simulations regardless of interatomic potentials, intrinsic defects, boundary conditions and model shapes. More importantly, IAMS makes the computational cost of MS simulations independent of simulation size, which is very attractive for extra-large scale simulations. These findings can help us to better understand energy minimization and how it affects the fidelity and efficiency of MS simulations.

6 Summary

In summary, the IAMS method based on atomic inertia effect is proposed to improve the efficiency of MS simulations. Design of the IAMS is inspired by mapping loading operation in MS simulations. By analyzing the results from MS simulations of simple 1D and 2D atomic systems, it is found that the mapping loading mode based on the knowledge of classical elastic solution can dramatically improve computational efficiency for MS simulations. Therefore, an update operation based on atomic inertia effect is introduced into IAMS to simulate mapping loading for more general systems regardless of shapes, boundary conditions and preexisting defects. It is done by self-learning from historical movements without knowledge of external loadings. Various simulations including compression of 2D atom bar, bending of different nanopillar and nanoindentation of 2D atom system are performed to validate the method. The results indicate that IAMS gains obvious efficiency improvement without loss of fidelity in comparison with conventional MS. Particularly, IAMS shows size-independent efficiency improvement. The upper limit of efficiency improvement of IAMS is also analyzed theoretically using different convergence precisions. Simplicity, generality and superior efficiency make IAMS a competitive method in MS simulations. IAMS also sheds light on improving other numerical methods such as large nonlinear deformation using finite element method and phase filed modeling.

Acknowledgments

Support from the National Key RD Program of China (2017YFB0202801), the National Natural Science Foundation of China (Grant nos. 11672298, 11432014 and 11790292), the Strategic Priority Research Program (B) of the Chinese Academy of Sciences (XDB22040501) is gratefully acknowledged. Computations are performed on the ScGrid of Supercomputing Center, Computer Network Information Center of Chinese Academy of Sciences.

References

[1] J. Li, K.J. Van Vliet, T. Zhu, S. Yip, S. Suresh, Atomistic mechanisms governing elastic limit and incipient plasticity in crystals, Nature. 418 (2002) 307310.
[2] X. Li, Y. Wei, L. Lu, K. Lu, H. Gao, Dislocation nucleation governed softening and maximum strength in nano-twinned metals, Nature. 464 (2010) 877880.
[3] Y. Wei, J. Wu, H. Yin, X. Shi, R. Yang, M. Dresselhaus, The nature of strength enhancement and weakening by pentagonheptagon defects in graphene, Nat. Mater. 11 (2012) 759763.
[4] L.A. Zepeda-Ruiz, A. Stukowski, T. Oppelstrup, V. V. Bulatov, Probing the limits of metal plasticity with molecular dynamics simulations, Nature. 550 (2017) 492495.
[5] S. Plimpton, Fast parallel algorithms for short-range molecular dynamics, J. Comput. Phys. 117 (1995) 119.

[6] V. Shastry, D. Farkas, Molecular statics simulation of fracture in -iron, Model. Simul. Mater. Sci. Eng. 4 (1996) 473492.
[7] B. Radhakrishnan, G.B. Sarma, T. Zacharia, Modeling the kinetics and microstructural evolution during static recrystallizationMonte Carlo simulation of recrystallization, Acta Mater. 46 (1998) 44154433.
[8] G. Henkelman, B.P. Uberuaga, H. Jnsson, A climbing image nudged elastic band method for finding saddle points and minimum energy paths, J. Chem. Phys. 113 (2000) 99019904.
[9] E.B. Tadmor, R.E. Miller, Modeling materials: continuum, atomistic, and multiscale techniques, Cambridge University Press, 2011.
[10] X. Li, Y. Wei, W. Yang, H. Gao, Competing grain-boundary- and dislocation-mediated mechanisms in plastic strain recovery in nanocrystalline aluminum., Proc. Natl. Acad. Sci. U. S. A. 106 (2009) 1610813.
[11] S. Weng, H. Ning, T. Fu, N. Hu, Y. Zhao, C. Huang, X. Peng, Molecular dynamics study of strengthening mechanism of nanolaminated graphene/Cu composites under compression, Sci. Rep. 8 (2018) 3089.
[12] S.T. Chill, M. Welborn, R. Terrell, L. Zhang, J.-C. Berthet, A. Pedersen, H. Jnsson, G. Henkelman, EON: software for long time simulations of atomic scale systems, Model. Simul. Mater. Sci. Eng. 22 (2014) 055002.
[13] J. Li, S. Sarkar, W.T. Cox, T.J. Lenosky, E. Bitzek, Y. Wang, Diffusive molecular dynamics and its application to nanoindentation and sintering, Phys. Rev. B. 84 (2011) 054103.
[14] P. Xiao, J. Wang, F.J. Ke, Y.L. Bai, Molecular statistical thermodynamics A distinct and efficient numerical approach to quasi-static analysis of nanomaterials at finite temperature, Compos. Part B Eng. 43 (2012) 5763.
[15] A.K. Subramaniyan, C.T. Sun, Engineering molecular mechanics: an efficient static high temperature molecular simulation technique, Nanotechnology. 19 (2008) 285706.
[16] M. Hu, H. Wang, M. Xia, F. Ke, Y. Bai, Cluster Statistical Thermodynamics (CST) To Efficiently Calculate Quasi-Static Deformation at Finite Temperature Based on Molecular Potential, in: IUTAM Symp. Mech. Behav. Micro-Mechanics Nanostructured Mater., Springer Netherlands, Dordrecht, 2007: pp. 163170.
[17] R.E. Miller, E.B. Tadmor, A unified framework and performance benchmark of fourteen multiscale atomistic/continuum coupling methods, Model. Simul. Mater. Sci. Eng. 17 (2009) 053001.
[18] J.J. Möller, A. Prakash, E. Bitzek, FE2ATfinite element informed atomistic simulations, Model. Simul. Mater. Sci. Eng. 21 (2013) 055011.
[19] E.B. Tadmor, M. Ortiz, R. Phillips, Quasicontinuum analysis of defects in solids, Philos. Mag. A. 73 (1996) 15291563.
[20] L.E. Shilkrot, R.E. Miller, W.A. Curtin, Multiscale plasticity modeling: coupled atomistics and discrete dislocation mechanics, J. Mech. Phys. Solids. 52 (2004) 755787.
[21] B. Shiari, R.E. Miller, Multiscale modeling of crack initiation and propagation at the nanoscale, J. Mech. Phys. Solids. 88 (2016) 3549.
[22] G. Anciaux, T. Junge, M. Hodapp, J. Cho, J.-F. Molinari, W.A. Curtin, The Coupled Atomistic/Discrete-Dislocation method in 3d part I: Concept and algorithms, J. Mech. Phys. Solids. 118 (2018) 152171.
[23] E. Bitzek, P. Koskinen, F. Ghler, M. Moseler, P. Gumbsch, Structural Relaxation Made Simple, Phys. Rev. Lett. 97 (2006) 170201.
[24] F. Shuang, P. Xiao, R. Shi, F. Ke, Y. Bai, Influence of integration formulations on the performance of the fast inertial relaxation engine (FIRE) method, Comput. Mater. Sci. 156 (2019)

135141.
[25] L. Yang, C. Hou, X. Ma, L. Ye, L. Chang, L. Shi, X. He, Structure relaxation via long trajectories made stable, Phys. Chem. Chem. Phys. 19 (2017) 2447824484.
[26] L. Mones, C. Ortner, G. Csnyi, Preconditioners for the geometry optimisation and saddle point search of molecular systems, Sci. Rep. 8 (2018) 13991.
[27] S.M. Foiles, M.I. Baskes, M.S. Daw, Embedded-atom-method functions for the fcc metals Cu, Ag, Au, Ni, Pd, Pt, and their alloys, Phys. Rev. B. 33 (1986) 79837991.
[28] A. Stukowski, Visualization and analysis of atomistic simulation data with OVITOthe Open Visualization Tool, Model. Simul. Mater. Sci. Eng. 18 (2010) 015012.
[29] A. Stukowski, Structure identification methods for atomistic simulations of crystalline materials, Model. Simul. Mater. Sci. Eng. 20 (2012) 045021.
[30] C.L. Kelchner, S.J. Plimpton, J.C. Hamilton, Dislocation nucleation and defect structure during surface indentation, Phys. Rev. B. 58 (1998) 1108511088.
[31] N. Jia, Y. Yao, Z. Peng, Y. Yang, S. Chen, Surface effect in axisymmetric Hertzian contact problems, Int. J. Solids Struct. 150 (2018) 241254.
[32] S. Goedecker, F. Lanon, T. Deutsch, Linear scaling relaxation of the atomic positions in nanostructures, Phys. Rev. B. 64 (2001) 161102.
[33] R.E. Miller, D. Rodney, On the nonlocal nature of dislocation nucleation during nanoindentation, J. Mech. Phys. Solids. 56 (2008) 12031223.
[34] T. Zhu, J. Li, K. J. Van Vliet, S. Ogata, S. Yip, S. Suresh, Predictive modeling of nanoindentation-induced homogeneous dislocation nucleation in copper, J. Mech. Phys. Solids. 52 (2004) 691724.
[35] F. Shuang, P. Xiao, F. Ke, Y. Bai, Efficiency and fidelity of molecular simulations relevant to dislocation evolutions, Comput. Mater. Sci. 139 (2017) 266272.
[36] V. V. Bulatov, L.L. Hsiung, M. Tang, A. Arsenlis, M.C. Bartelt, W. Cai, J.N. Florando, M. Hiratani, M. Rhee, G. Hommes, T.G. Pierce, T.D. De La Rubia, Dislocation multi-junctions and strain hardening, Nature. 440 (2006) 11741178.
[37] W.B. Gragg, H.J. Stetter, Generalized Multistep Predictor-Corrector Methods, J. ACM. 11 (1964) 188209.
[38] D.C. Liu, J. Nocedal, On the limited memory BFGS method for large scale optimization, Math. Program. 45 (1989) 503528.
[39] X. Tan, J. Wu, K. Zhang, X. Peng, L. Sun, J. Zhong, Nanoindentation models and Youngs modulus of monolayer graphene: A molecular dynamics study, Appl. Phys. Lett. 102 (2013) 071908.
[40] Z. Dai, G. Wang, Z. Zheng, Y. Wang, S. Zhang, X. Qi, P. Tan, L. Liu, Z. Xu, Q. Li, Z. Cheng, Z. Zhang, Mechanical responses of boron-doped monolayer graphene, Carbon N. Y. 147 (2019) 594601.
[41] J.A. Stewart, D.E. Spearot, Atomistic simulations of nanoindentation on the basal plane of crystalline molybdenum disulfide (MoS 2), Model. Simul. Mater. Sci. Eng. 21 (2013) 045003.
[42] Z. Dai, L. Liu, Z. Zhang, Strain Engineering of 2D Materials: Issues and Opportunities at the Interface, Adv. Mater. (2019) 1805417.
[43] Z. Dai, Y. Hou, D.A. Sanchez, G. Wang, C.J. Brennan, Z. Zhang, L. Liu, N. Lu, Interface-Governed Deformation of Nanobubbles and Nanotents Formed by Two-Dimensional Materials, Phys. Rev. Lett. 121 (2018) 266101.
[44] E.L. Allgower, K. Georg, Continuation and path following, Acta Numer. 2 (1993) 164.
[45] J. Brindley, C. Kaas-Petersen, A. Spence, Path-following methods in bifurcation problems, Phys. D Nonlinear Phenom. 34 (1989) 456461.

[46] A. Maghami, F. Shahabian, S.M. Hosseini, Path following techniques for geometrically nonlinear structures based on Multi-point methods, Comput. Struct. 208 (2018) 130142.
[47] N.A. Labanda, S.M. Giusti, B.M. Luccioni, A path-following technique implemented in a Lagrangian formulation to model quasi-brittle fracture, Eng. Fract. Mech. 194 (2018) 319336.
[48] A. Fayezioghani, B. Vandoren, L.J. Sluys, Performance-based step-length adaptation laws for path-following methods, Comput. Struct. 223 (2019) 106100.
[49] J. Chen, P. Ming, An Efficient Multigrid Method for Molecular Mechanics Modeling in Atomic Solids, Commun. Comput. Phys. 10 (2011) 7089.